Title

Arap1 Deficiency Causes Photoreceptor Degeneration in MiceArap1 Deficiency Causes Photoreceptor Degeneration

Permalink

https://escholarship.org/uc/item/5g2402kd

Journal

Investigative Ophthalmology & Visual Science, 58(3)

ISSN

0146-0404

Authors

Moshiri, Ala
Humpal, Devin
Leonard, Brian C
et al.

Publication Date

2017-03-21

DOI

10.1167/iovs.16-20062

Peer reviewed

Arap1 Deficiency Causes Photoreceptor Degeneration in Mice

Ala Moshiri,[1] Devin Humpal,[1] Brian C. Leonard,[2] Denise M. Imai,[3] Addy Tham,[1] Lynette Bower,[4] Dave Clary,[4] Thomas M. Glaser,[5] K. C. Kent Lloyd,[4] and Christopher J. Murphy[1,2]

[1]Department of Ophthalmology and Vision Science, School of Medicine, U.C. Davis, Sacramento, California, United States
[2]Department of Veterinary Surgical and Radiological Sciences, School of Veterinary Medicine, U.C. Davis, Davis, California, United States
[3]Comparative Pathology Laboratory, U.C. Davis, Davis, California, United States
[4]Mouse Biology Program, U.C. Davis, Davis, California, United States
[5]Department of Cell Biology and Human Anatomy, U.C. Davis, Davis, California, United States

PURPOSE. Small guanosine triphosphatase (GTPase) ADP-ribosylation factors (Arfs) regulate membrane traffic and actin reorganization under the control of GTPase-activating proteins (GAPs). *Arap1* is an Arf-directed GAP that inhibits the trafficking of epidermal growth factor receptor (EGFR) to the early endosome, but the diversity of its functions is incompletely understood. The aim of this study was to determine the role of *Arap1* in the mammalian retina.

METHODS. Genetically engineered *Arap1* knockout mice were screened for ocular abnormalities in the National Institutes of Health Knockout Mouse Production and Phenotyping (KOMP2) Project. *Arap1* knockout and wild-type eyes were imaged using optical coherence tomography and fundus photography, and analyzed by immunohistochemistry.

RESULTS. *Arap1*$^{-/-}$ mice develop a normal appearing retina, but undergo photoreceptor degeneration starting at 4 weeks postnatal age. The fundus appearance of mutants is notable for pigmentary changes, optic nerve pallor, vascular attenuation, and outer retinal thinning, reminiscent of retinitis pigmentosa in humans. Immunohistochemical studies suggest the cell death is predominantly in the outer nuclear layer. Functional evaluation of the retina by electroretinography reveals amplitudes are reduced. *Arap1* is detected most notably in Müller glia, and not in photoreceptors, implicating a role for Müller glia in photoreceptor survival.

CONCLUSIONS. *Arap1* is necessary for normal photoreceptor survival in mice, and may be a novel gene relevant to human retinal degenerative processes, although its mechanism is unknown. Further studies in this mouse model of retinal degeneration will give insights into the cellular functions and signaling pathways in which *Arap1* participates.

Keywords: retinitis pigmentosa, rod-cone degeneration, photoreceptors

Retinitis pigmentosa (RP) is the leading cause of inherited blindness.[1] It is a retinal degenerative disease caused by the death of photoreceptors, and occurs in approximately 1 of 4000 people during their lifetime,[2] with an estimated 1.5 million people affected worldwide. Patients in the early stages of RP often detect problems seeing in dim light, as well as loss of peripheral vision. These symptoms correspond to the loss of rod photoreceptors, which predominate in the peripheral human retina, and are required for visual functioning in low light levels. Following the death of rods, cone photoreceptors and retinal pigment epithelium (RPE) cells die secondarily. Eventually the macula is affected as well, and in the end stage of the disease all vision is lost. Retinitis pigmentosa is a clinical diagnosis with characteristic bone spicule hyperpigmentation in the retinal periphery, retinal vascular attenuation, pallor of the optic nerve, and RPE atrophy in areas in which rods have been lost. Currently there is no treatment to restore vision, or to slow progression of vision loss. Artificial retinal implants, retinal transplantation, stem cell therapy, gene editing, systemic medications, and vitamin supplements are all areas of active research. Understanding the full complement of pathways that can lead to the pathogenesis of RP is important to developing potential therapeutic strategies.

Mutations in more than 60 genes have been linked to nonsyndromic RP, 35 of which cause recessive disease.[3] Causative genetic mutations usually fall into a few categories of rod photoreceptor function, such as phototransduction, outer segment (ciliary) protein trafficking, disk formation and stabilization, ATP production, lipid metabolism, and the visual cycle. Because rod photoreceptors depend on RPE cells to regenerate photopigment as part of the visual cycle, as well as for rod outer segment phagocytosis, mutations inhibiting either of these two RPE functions account for some cases of RP.

In an effort to discover novel mutations causing eye disease, systematic ophthalmic screening was performed on every mouse line as part of the Knockout Mouse Production and Phenotyping (KOMP2) Project in the International Mouse Phenotyping Consortium conducted at the University of

Investigative Ophthalmology & Visual Science

California (U.C.) Davis Mouse Biology Program. Mice deficient in *Arap1* were generated using embryonic stem cells with a homozygous knockout of this gene from the European Conditional Mouse Mutagenesis Program. Retinal abnormalities were identified during comprehensive ophthalmic screening, and detailed investigation revealed that *Arap1*$^{-/-}$ mice undergo a progressive retinal degeneration similar to RP in humans. The fundus of these animals developed pigmentary changes, retinal vascular attenuation, optic nerve pallor, and outer retinal thinning reminiscent of the analogous disease in humans. The retina developed all neuronal cell types with appropriate lamination and morphology, and began to degenerate in young adulthood, similar to the onset of disease in typical recessive human cases of RP. Most cell death is limited to the photoreceptor layer, and ERG amplitudes are correspondingly reduced.

The function of *Arap1* in the retina is unclear. In general, small guanosine triphosphatase (GTPase) ADP-ribosylation factors (Arfs) regulate membrane traffic and actin reorganization under the control of GTPase-activating proteins (GAPs). *Arap1* is an Arf-directed GAP that inhibits the progression of epidermal growth factor receptor (EGFR) to the early endosome, but the diversity of its functions is poorly understood. *Arap1* has multiple pleckstrin homology (PH) domains that recognize phosphatidylinositol 3,4,5-trisphosphate. It can be located near the Golgi apparatus or at the plasma membrane in certain cell types, and has been shown to regulate members of the Arf and Rho small GTPase protein families in vitro. Whether *Arap1* regulates cellular processes in the retina through one or more of the above mechanisms, and/or via other molecular partners remains to be determined.

METHODS

This study was conducted according to a protocol that was approved by the Institutional Animal Care and Use Committee at U.C. Davis and was compliant with the ARVO Statement for the Use of Animals in Ophthalmic and Vision Research.

Animals

Mice were generated by the U.C. Davis Mouse Biology Program using embryonic stem cells with a homozygous knockout of *Arap1* obtained from the European Conditional Mouse Mutagenesis Program by the KOMP2 Project as part of the International Mouse Phenotyping Consortium. A targeting cassette with a *LacZ* insert was used to knock out exon 9 of the *Arap1* gene. This causes a frameshift in every protein-coding transcript of the gene, making residual transcript subject to nonsense mediated decay. Heterozygous *Arap1*$^{+/-}$ mice were generated on a C57BL/6N background, and intercrossed to establish homozygous male and female cohorts for initial phenotypic screening. The weight, development, growth, and behavior of the knockout animals appeared grossly normal. Necropsy of mutant animals by veterinary pathologists in the KOMP2 pipeline identified tibial dysplasia, abnormal caudal vertebra morphology, and decreased lean body mass (www.impc.org). For secondary, in-depth ocular phenotyping, *Arap1*$^{+/-}$ founders were crossed with wild-type C57BL/6J animals to establish mutant mice free from the confounding rd8 mutation common in the 6N strain, as confirmed by PCR genotyping for rd8. A research colony was bred crossing heterozygotes to produce homozygous mutants and wild-type control littermates for this study. The animals were maintained at the Teaching and Research Animal Care Services facility at U.C. Davis. Genotyping primers targeted the *LacZ* insert and exon 9 region: LacZ-F ACACTACGTCT GAACGTCGAAAACCCGAAACT; LacZ-R CAGACGATTCATTGG CACCATGCCGTG; Arap1-F CCGGTTCTACTTATGTGTCCCTAG CTTCTCGG; and Arap1-R TTAGATATAAGGGCTGTAGGGATCTG CCCAGCAGA. At time points relevant to retinal development and progression of retinal degeneration, animals were euthanized by isoflurane inhalation followed by cervical dislocation.

Indirect Ophthalmoscopy

Mice were screened by a veterinary ophthalmologist (B.C.L.) at 16 weeks postnatal age with a handheld 60-diopter lens. Seven male and seven female homozygous *Arap1* knockout mice and two male and two female wild-type littermates were evaluated in a blinded fashion. All animals that were part of the original screening process were on the C57BL/6N background.

Electroretinography

Mice were dark-adapted overnight and anesthetized with an intraperitoneal injection of a ketamine/dexmedetomidine (50–75/0.25–0.5 mg/kg) cocktail. Eyes were dilated with 1% tropicamide (Bausch + Lomb, Rochester, NY, USA) and 2.5% phenylephrine hydrochloride (Paragon, Portland, OR, USA). 2.5% hypromellose (OCuSOFT, Rosenberg, TX, USA) and GenTeal Gel (Novartis, Sacramento, CA, USA) were used as eye lubricant. Full-field ERG was used to test scotopic retinal function (white flashes of 0.001, 0.01, 0.1, 1.0, 2.5, and 10.0 cd*s/m^2) and, after 10 minutes of light adaptation (30 cd/m^2), photopic retinal function (white flashes of 0.1, 0.4, 1.0, 2.5, and 10.0 cd*s/m^2). Stimuli were generated by a Ganzfeld stimulator (UTAS Visual Diagnostic System with BigShot LED; LKC Technologies, Gaithersburg, MD, USA). Responses were referenced and grounded to needle electrodes between the ears and the lower back, respectively. Dexmedetomidine was reversed with atipamezole (0.25–0.5 mg/kg). B-wave amplitudes were measured from the trough of the a-wave to the peak of the third oscillatory potential past the resting potential.

Fundus Photography and Optical Coherence Tomography

Mice were anesthetized with an intraperitoneal injection of a ketamine/midazolam (50–75/1–2 mg/kg) cocktail. Eyes were dilated with tropicamide 1% and phenylephrine 2.5% drops, and lubricated with methylcellulose. Fundus photographs were taken with the Micron III (Phoenix Research Laboratories, Pleasanton, CA, USA), and spectral-domain optical coherence tomography (OCT) images were taken with the Envisu R2200 (Bioptigen, Morrisville, NC, USA) at 14 to 18 weeks postnatal age.

Immunohistochemistry and X-Gal Staining

Eyes were enucleated and then fixed in 4% paraformaldehyde for 20 minutes at room temperature. Cornea and lens were removed; eyecups were then cryoprotected in a 10%–20%–30% sucrose gradient (4°C) for at least 1 hour at each concentration. Eyecups were embedded in optimum cutting temperature medium (Thermo Fisher Scientific, Waltham, MA, USA), frozen in dry ice and 2-methylbutane slurry, and sectioned at 10 µm onto Superfrost Plus (Thermo Fisher) slides with a cryostat (LEICA CM3050; Leica, Wetzlar, Hesse, Germany).

For immunohistochemistry, slides were washed with 1× PBS (10 mM phosphate, 137 mM NaCl, 2.7 mM KCl), sections were circled with a PAP pen (Ted Pella, Redding, CA, USA) and blocked with 1% to 3% BSA in 0.3% Triton X-100 in PBS for 3 hours at room temperature. Sections were incubated in primary antibody overnight (4°C), washed in PBS, and then
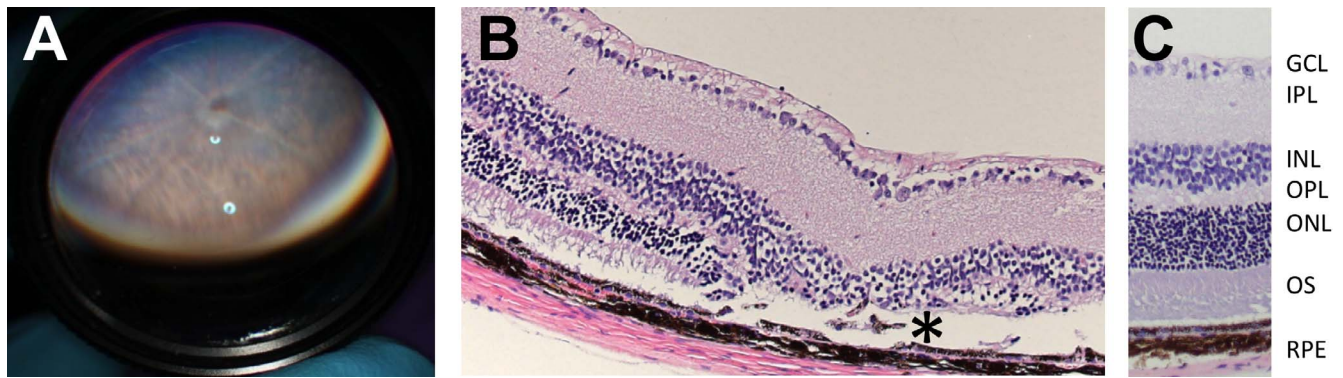
FIGURE 1. *Arap1*^{−/−} animals were clinically identified and histologically confirmed by screening knockout mice in the KOMP2 production and phenotyping line. *Arap1*^{−/−} and age-matched wild-type C57BL/6N mice were examined by indirect ophthalmoscopy using a 60-diopter lens (**A**) demonstrating pigmentary abnormalities and atrophic lesions in *Arap1*^{−/−} animals, much more so than in C57BL/6N *Arap1*^{+/+} mice (not shown). Histology (hematoxylin-eosin stain) of *Arap1*^{−/−} mice at 16 weeks postnatal (**B**) showed outer retinal dysplasia and areas of missing photoreceptors (*), when compared with wild-type C57BL/6N mice (**C**). The ganglion cell layer (GCL), inner plexiform layer (IPL), inner nuclear layer (INL), outer plexiform layer (OPL), outer nuclear layer (ONL), outer segments (OS), and RPE are labeled.

incubated with the matching secondary antibody for 2 hours at room temperature, washed in PBS, and then coverslipped with FluorSave (Calbiochem, Temecula, CA, USA) and imaged. Primary antibodies included rabbit anti-activated Caspase-3 (1:200, 559565; BD Biosciences, San Jose, CA, USA), mouse anti-Pax6 (1:100; Developmental Studies Hybridoma Bank, Iowa City, IA, USA), goat anti-Otx2 (1:300, BAF1979; R&D Systems, Minneapolis, MN, USA), rabbit anti-Glutamine synthetase (1:1000, G2781; Sigma-Aldrich Corp., St. Louis, MO, USA), and rat anti-β galactosidase (1:500, gift from Tom Glaser).[4] Secondary antibodies (AlexaFluor) included 488 donkey anti-rabbit (1:200, A21206; Life Technologies, Carlsbad, CA, USA), 568 donkey anti-mouse (1:300, A10037; Life Technologies), 488 donkey anti-goat (1:300, 705-545-147; Jackson Immuno Research, West Grove, PA, USA), and 488 goat anti-rat (1:300, A-11006; Thermo Fisher).

For colabeling experiments, eyes were enucleated and rapidly frozen by immersion in dry ice-cooled liquid propane for 30 seconds,[5] and transferred to glass vials containing 97% methanol and 3% acetic acid (M-AA) held at dry ice temperatures. The glass vial with the eyes was placed at −80°C for 48 hours. After 48 hours, the vial was warmed stepwise by 4-hour stops at −40°C and −20°C, and then at room temperature for 48 hours. After 48 hours at room temperature, the M-AA was replaced with three changes of 100% ethanol, for 15 minutes each, then two 15-minute changes of 100% xylene, then three 45-minute changes of 60°C paraffin. Sections 4 μm in thickness were harvested using a Leica microtome. Sections were de-paraffinized, placed into a slide chamber and filled with 0.01 M sodium citrate diluted in PBS. Slides were then heated in a 700-watt microwave for 10 seconds and then cooled at room temperature for 5 minutes before heating again for 10 seconds. Immediately after, fresh sodium citrate solution was replaced in the chamber and the process was repeated once more. Sections were blocked as above, and incubated overnight (4°C) with both primary antibodies, followed by five 5-minute washes in PBS, and then incubated with the matching secondary antibodies for 2 hours at room temperature, washed in PBS, exposed to 4′,6-diamidino-2-phenyl-indole (DAPI) in PBS for 5 minutes for nuclear localization, washed, and then coverslipped with FluorSave (Calbiochem) and imaged.

For X-gal staining, cryosections were washed with PBS and then incubated in the dark at 37°C in X-gal stain (1.5 mM potassium ferricyanide and potassium ferrocyanide, 1.3 mM

magnesium chloride, and 25 mg X-gal dissolved in dimethyl-formamide for a total volume of 1.25 mL, all in PBS) for 18 to 48 hours. After a PBS wash, slides were coverslipped with Vectamount (Vector Laboratories, Burlingame, CA, USA) and imaged.

Histology

Eyes were enucleated and then immediately oriented in optimum cutting temperature medium and frozen in liquid nitrogen. Cryosections were prepared as described above. Sections were treated with cold acetone, hematoxylin, 0.5% HCl in 70% ethanol, eosin, 95% and 100% ethanol, and Histo-Clear (National Diagnostics, Atlanta, GA, USA). Slides were coverslipped with Vectamount and imaged.

Statistical Analysis

For all quantification, at least three animals ($n = 3$) were imaged for each genotype and each age. Images were obtained from at least three sections for each animal, and measurements for each animal were combined to determine the average measurement for each animal. These values were then averaged with the other animals in each group. Pairwise analyses were done using the Student's t-test; P values of 0.05 or less were considered statistically significant.

Imaging

Immunohistochemistry, X-gal staining, and histology slides were all imaged using a Nikon (Melville, NY, USA) Eclipse E800 microscope with an X-Cite (Waltham, MA, USA) 120–light-emitting diode fluorescence source and Q Capture Pro 7 software (Surrey, BC, Canada).

RESULTS

Arap1^{−/−} Mice Undergo Degeneration of the Outer Nuclear Layer

Veterinary ophthalmology team members examined animals at 16 weeks postnatal age as part of the KOMP2 project conducted by the U.C. Davis Mouse Biology Program by indirect ophthalmoscopy with the aid of a handheld 60-diopter lens (Fig. 1A). The phenotyping examiner (BCL) was presented 18 animals at the same time in a blinded fashion. These
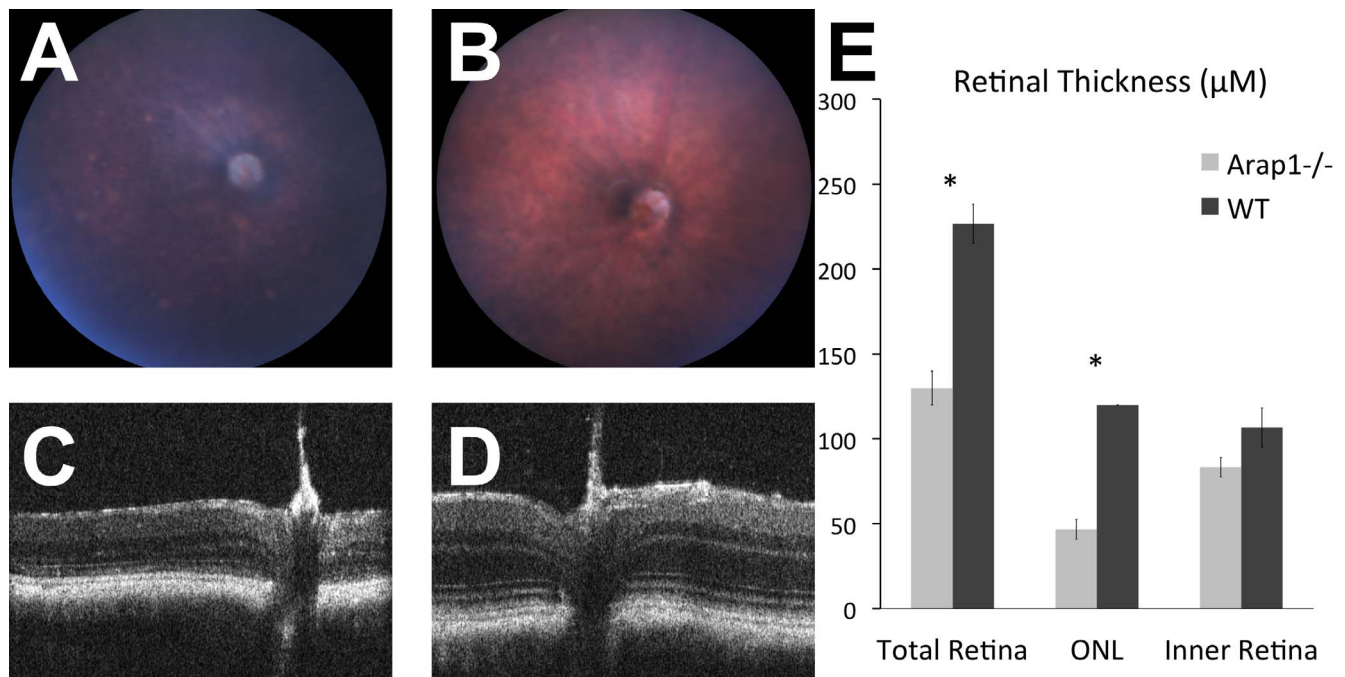
Figure 2. *Arap1*$^{-/-}$ mice had photoreceptor degeneration independent of *rd8*. *Arap1*$^{-/-}$ fundus (**A**) at 14 weeks postnatal had nerve pallor, pigmentation changes, and vessel attenuation compared with wild type (**B**). Optical coherence tomography at 14 weeks postnatal showed thinned ONL in *Arap1*$^{-/-}$ (**C**) compared with wild type (**D**). Manual segmentation quantifying the retinal thickness of OCT layers (**E**) from animals 14 to 18 weeks postnatal age confirmed the thinning is in the ONL ($n = 3$ each group, *$P < 0.05$, *error bars* represent SE).

consisted of seven male and seven female homozygous knockout animals, and two male and two female wild-type littermates. The retinal degeneration phenotype identified by fundoscopy segregated with animal genotype. The original histology was performed by U.C. Davis veterinary pathologists. They reported thinning and dysplasia of the photoreceptor layer of the retina of *Arap1*$^{-/-}$ animals (Fig. 1B) when compared with wild-type animals (Fig. 1C). The original knockout mice (Fig. 1) were generated on a C57BL/6N background bearing the rd8 mutation. To better study the role of *Arap1* in the retina, *Arap1*$^{+/-}$ animals were crossed with wild-type C57BL/6J mice and then heterozygous intercrossed to establish a homozygous colony free from the confounding rd8 mutation common in the 6N strain. All subsequent figures show data independent of rd8.

The fundus appearance of adult *Arap1*$^{-/-}$ mice showed changes typical of mouse models of RP. By age 14 weeks, the fundus exhibited optic nerve pallor, attenuated retinal arteries, retinal pigmentary changes, and focal areas of RPE atrophy (Fig. 2A), features that were not present in wild-type littermates (Fig. 2B). Consistent with the histopathology, the OCT performed on these eyes showed profound thinning of the outer retina with relative preservation of the inner retina in *Arap1*$^{-/-}$ mice (Fig. 2C) in comparison with the OCT of wild-type littermates (Fig. 2D). To determine which layers of the retina were abnormal, manual segmentation of the OCT of *Arap1*$^{-/-}$ mice ($n = 3$) and wild-type littermates ($n = 3$) was performed. The total retinal thickness on OCT was measured on single line scans at the level of the optic nerve. The thickness of the photoreceptor layer was also measured, as well as the thickness of the inner retinal layers. Our OCT measurements indicate a marked thinning of the retina by 14 to 18 weeks postnatal in *Arap1*$^{-/-}$ mice. The result of the OCT segmentation shows the retinal thinning is predominantly in the photoreceptor layer, as the inner retina in *Arap1*$^{-/-}$ mice at this age is similar to controls (Fig. 2E).

Arap1 Is Not Required for Retinal Histogenesis

To distinguish if *Arap1*$^{-/-}$ mice fail to generate appropriate numbers of photoreceptors, or if they have normal retinal histogenesis followed by photoreceptor degeneration, animals were killed just after retinal development ended, and eyes were taken for more detailed histologic analysis. *Arap1*$^{-/-}$ retinas at 2 weeks postnatal were sectioned and stained with hematoxylin and eosin, which demonstrated similar retinal lamination and thickness when compared with wild-type controls (Figs. 3A, 3E). However, when animals were examined at 4, 6, and 8 weeks postnatal, the outer nuclear layer of *Arap1*$^{-/-}$ mice had progressively degenerated (Figs. 3B–D), whereas control retinas had not (Figs. 3F–H). Quantification of the retinal lamination between *Arap1*$^{-/-}$ and wild-type controls demonstrated no significant difference between any of the layers of the retina at 2 weeks postnatal age (Supplementary Figs. S1A–G). However, at postnatal weeks 4, 6, and 8, we measured a progressive thinning of the outer nuclear layer in *Arap1*$^{-/-}$ mice (Supplementary Fig. S1E). By 8 weeks postnatal, we observed some thinning of the retinal ganglion cell layer, inner nuclear layer, and outer plexiform layer (Supplementary Figs. S1A, S1C, S1D, respectively), which may be secondary to the primary photoreceptor degeneration. The thickness of the photoreceptor inner/outer segments was consistently less in *Arap1*$^{-/-}$ mice at all ages examined (Supplementary Fig. S1F).

To test if various retinal cell types are generated appropriately in the *Arap1*-deficient retina, retinal sections from 2 weeks postnatal mice were stained for retinal ganglion cells and amacrine cells using antibodies against the transcription factor Pax6. *Arap1*$^{-/-}$ retinal sections marked for Pax6 (Fig. 4A) demonstrated that these cell types were generated in similar density and pattern as wild-type control retinas (Fig. 4B). The staining pattern of Pax6-positive cells remained similar between knockout and control mice at 8 weeks postnatal age
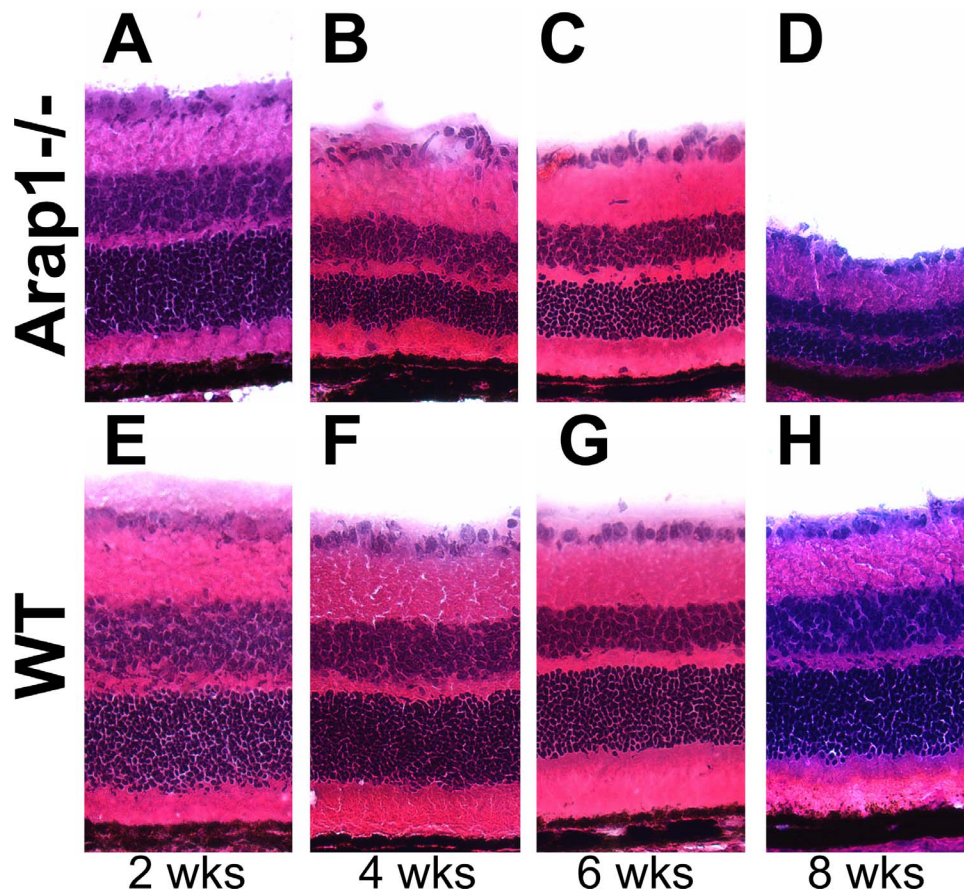
FIGURE 3. $Arap1^{-/-}$ mice undergo progressive photoreceptor degeneration. Hematoxylin-eosin staining of representative retinal sections of $Arap1^{-/-}$ (**A–D**) and WT (**E–H**) animals are shown. $Arap1^{-/-}$ animals at 2 weeks postnatal age (**A**) showed similar retinal lamination and anatomy to wild-type (**E**) animals. However, progressive outer retinal thinning at weeks 4 (**B**), 6 (**C**), and 8 (**D**) postnatal age in $Arap1^{-/-}$ mice demonstrated the photoreceptor layer had degenerated substantially compared with wild-type animals (**F**, **G**, **H**). Quantification of retinal laminar thicknesses at these stages is shown in Supplementary Figure S1.

(Figs. 4C, 4D), suggesting no obvious loss of these inner retinal cell types.

Bipolar neurons and photoreceptors were stained using the marker Otx2. At 2 weeks postnatal, the number and location of these cell types appeared grossly indistinguishable between $Arap1^{-/-}$ (Fig. 4E) and wild-type mice (Fig. 4F). However, by 8 weeks postnatal age, the Otx2-positive photoreceptor layer had markedly thinned in $Arap1^{-/-}$ mice (Fig. 4G) when compared with wild-type mice at the same age (Fig. 4H).

Arap1 Is Expressed in the Retina and Is Required for Photoreceptor Survival

Taking advantage of the LacZ cassette knocked into the *Arap1* locus and under the control of its promoter, a histochemical reaction was performed to determine the expression pattern of *Arap1* in the retina. Blue signal from the X-gal reagent was seen in the retinal ganglion cell layer, inner nuclear, and in the outer nuclear layer at 4 weeks postnatal age in $Arap1^{+/-}$ (Fig. 5A) and $Arap1^{-/-}$ mice (Fig. 5B). Surprisingly, few cells in the outer nuclear layer expressed LacZ. Similarly, only a few cells in the RPE layer showed a positive signal. The reagent did not give a signal in control retina at the same age (Fig. 5C).

Immunohistochemistry was performed using a primary antibody against β-galactosidase, and the pattern of reactivity was reminiscent of a Müller glial staining pattern. Colabeling experiments confirmed that β-galactosidase immunolabeling

coincided with glutamine synthetase signal in Müller cells in $Arap1^{+/-}$ (Figs. 5E, 5E', 5E'') and $Arap1^{-/-}$ mice (Figs. 5F, 5F', 5F''), but not in wild-type controls (Figs. 5D, 5D', 5D'').

To determine if photoreceptor cells were being lost due to programmed cell death, immunohistochemistry was performed against activated Caspase-3. Retinal sections from mice at 4 weeks postnatal age showed the highest number of immunoreactive cells (Fig. 6A), all of which localized to the outer nuclear layer, and were in a distribution consistent with mainly rod photoreceptor death. Programmed cell death is limited to just the occasional cell in wild-type control retina (Fig. 6B). The vast majority of apoptosis was observed to take place between postnatal day 27 and 33 in $Arap1^{-/-}$ mice, and was quantified at 4 weeks postnatal (Fig. 6C). Activated Caspase-3 immunoreactivity was not seen in $Arap1^{-/-}$ retina at 2 weeks postnatal, and seemed to decrease to only an occasional cell by 8 weeks postnatal age (data not shown).

We performed ERG on $Arap1^{-/-}$ mice to determine if they have decreased retinal activity. We found that $Arap1^{-/-}$ mice had reduced amplitudes in scotopic and photopic ERG conditions. Flash-response functions are shown from $Arap1^{-/-}$ mice at postnatal day 24 and age-matched controls (Fig. 7A). At this stage, the a-wave and b-wave in both groups are similar in amplitude. At later stages in the degeneration (15–18 weeks), both the a-wave and b-wave amplitudes are consistently reduced in $Arap1^{-/-}$ mice (Fig. 7B). The photopic responses were reliable only at the highest stimulus level (10 cd*s/m²). The b-wave amplitude at this stimulus level was relatively
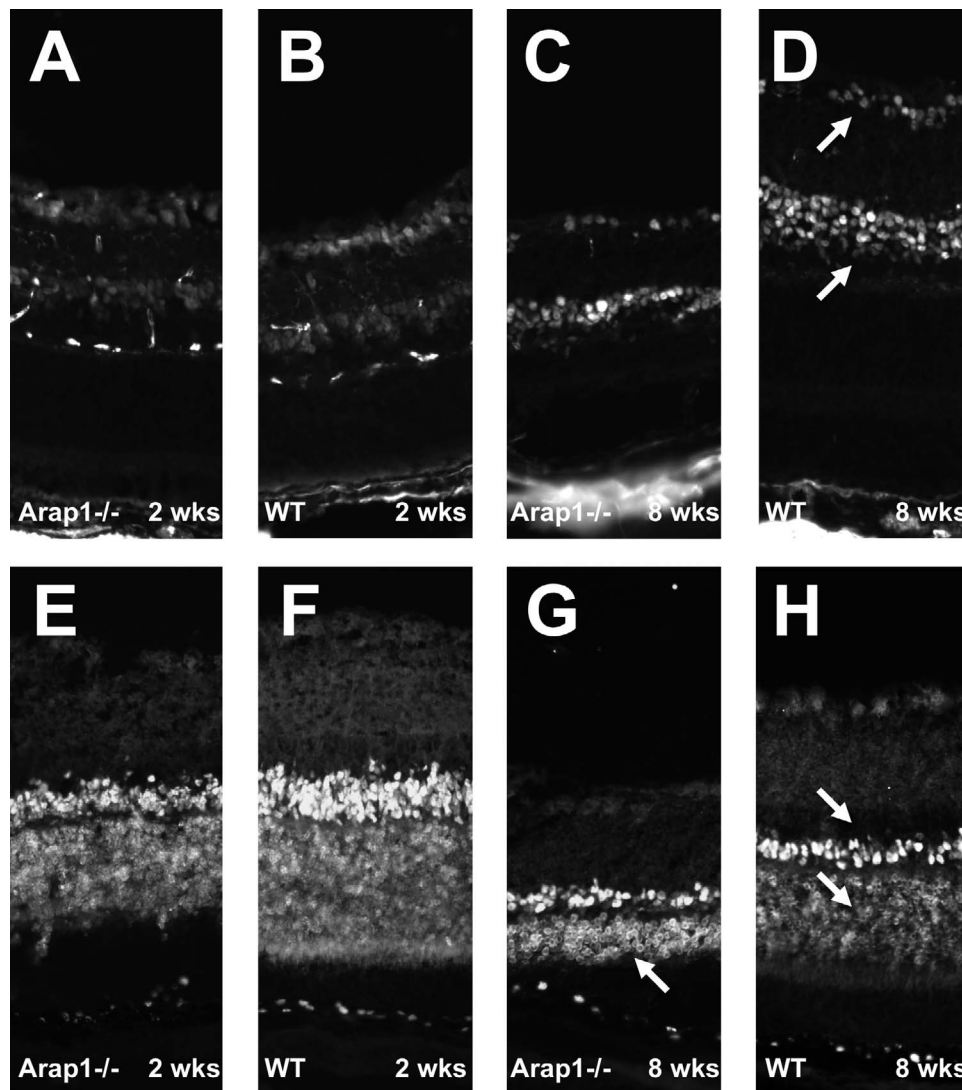
FIGURE 4. *Arap1⁻/⁻* mice form appropriate numbers and types of laminated retinal neurons. Immunohistochemistry using anti-Pax6 was performed to mark retinal ganglion cells and amacrine cells (*arrows* in [**D**]). *Arap1⁻/⁻* retina from 2 weeks postnatal mice (**A**) showed a similar staining pattern as wild-type (**B**) animals at this age. Anti-Otx2 labeling was used to mark bipolar and photoreceptor cells (*arrows* in [**H**]). A similar pattern of Otx2 staining was seen between *Arap1⁻/⁻* (**E**) and wild-type (**F**) controls at 2 weeks postnatal age. By 8 weeks of age, the Pax6 labeling in the degenerating *Arap1⁻/⁻* retina (**C**) remained similar to controls (**D**); however, the Otx2-labeled photoreceptor layer was markedly thin by 8 weeks in *Arap1⁻/⁻* mice (*arrow*, **G**) when compared with wild-type controls (*lower arrow*, **H**).

preserved in *Arap1⁻/⁻* mice both early and in late stages (Fig. 7C).

DISCUSSION

The findings in this study demonstrate that *Arap1* is required for the survival of photoreceptors in the mouse. The retinal developmental program appears to proceed normally in producing various retinal neurons with appropriate lamination by 2 weeks postnatal age. By postnatal day 27, massive apoptosis is observed in the outer nuclear layer, which proceeds actively through postnatal day 33 before slowing down to a very low level thereafter. Surprisingly, before and after the fifth week of life, which represents the peak of cell death, much less apoptosis is seen. It is possible that the thinning of the outer nuclear layer, which takes place well after the apoptotic markers decline, is in part due to removal of already dead photoreceptors. It is difficult to determine

definitively from the ERG data obtained which photoreceptors, rods or cones, are affected primarily. The relative preservation of the photopic b-wave suggests the cones may be less dependent on *Arap1* than rods, but more detailed analysis of the apoptotic cells with colabeling experiments will be required to clarify this issue.

In 2002, the laboratory of Paul Randazzo discovered Arf GAP, Rho GAP, Ankyryn repeat, and Pleckstrin homology protein 1 (*ARAP1*), and it was initially proposed to function at a potential crossing point between Arf- and Rho-GTPase signaling.[6] *ARAP1* is a member of the *AZAP* family of Arf GAPs (*ASAP*s, *ACAP*s, *AGAP*s, and *ARAP*s), which contain an Arf GAP domain, Rho GAP domain, sterile alpha motif (SAM), ankyrin repeat, five PH domains, and Ras association (RA) domain. The Arf GAP activity of *ARAP1* is stimulated in vitro by the binding of phosphatidylinositol 3,4,5-trisphosphate $(PI[3,4,5]P_3)$.[7] It was found to be associated with the plasma membrane, Golgi, in vesicles, and promoting recycling of endocytosed EGFR, hence potentiating EGFR signaling.[8] It is
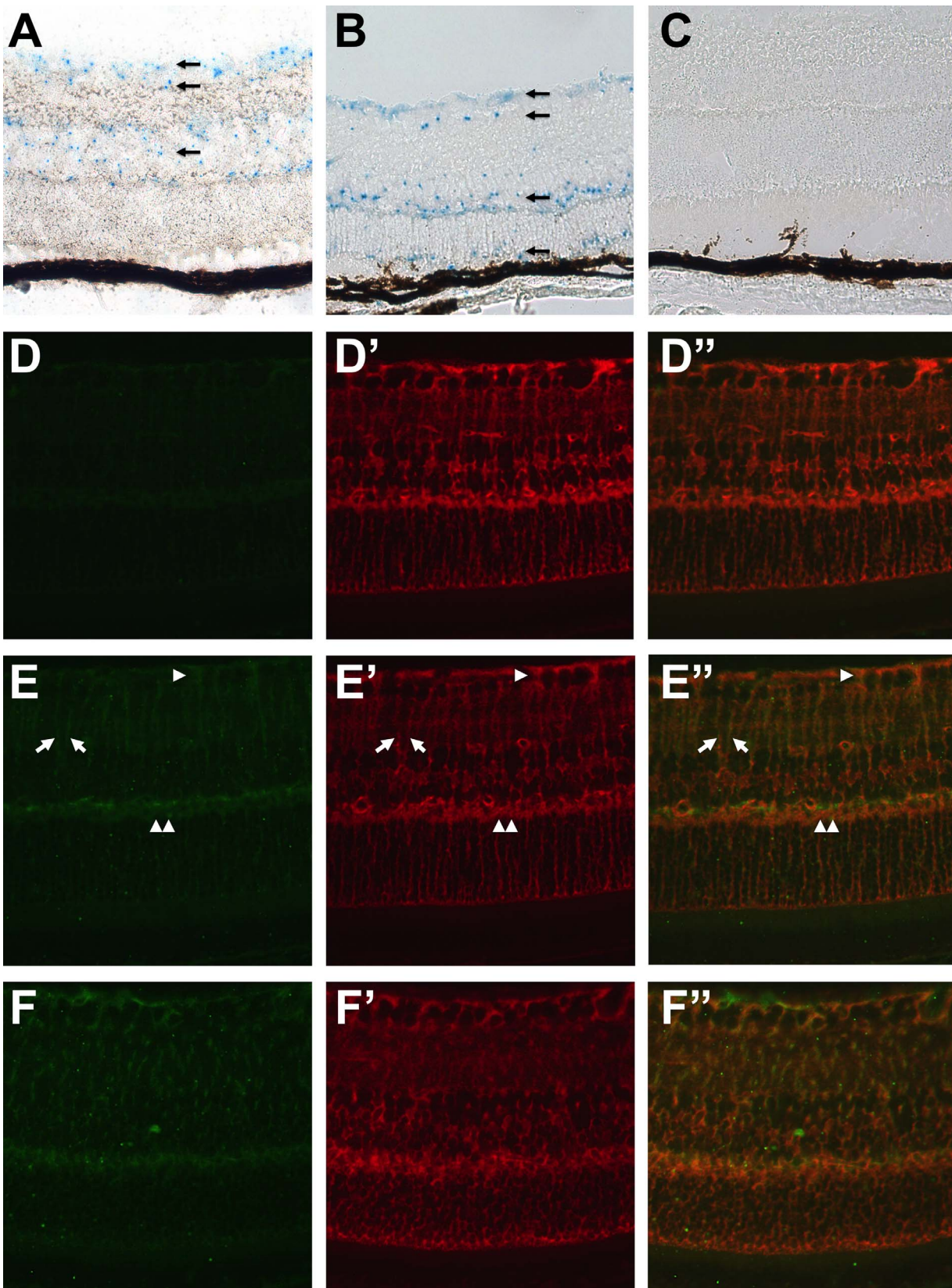
FIGURE 5. *Arap1* is expressed in Müller glia. LacZ histochemical reaction using X-gal reagent showed faint blue staining in the retinal GCL, INL, and in the ONL (*arrows*) in the *Arap1*$^{+/-}$ (**A**) and *Arap1*$^{-/-}$ (**B**) retina at 4 weeks postnatal age. There was sporadic staining in a few cells in the RPE. Control wild-type littermates showed no staining (**C**). Immunohistochemistry for β-galactosidase showed no staining in wild-type retina at 6 weeks (**D**). Glutamine synthetase labeling (**D'**) highlighted Müller cells (*red*), and the merged image is shown (**D''**). In 6-week-old *Arap1*$^{+/-}$ (**E**) and *Arap1*$^{-/-}$ (**F**) mice, β-galactosidase labeling is seen (*green*) in a pattern reminiscent of Müller cell staining. Colabeling with glutamine synthetase (*Arap1*$^{+/-}$ in [**E'**]; *Arap1*$^{-/-}$ in [**F'**]) confirms colocalization with β-galactosidase in Müller glia. Merged images are shown for *Arap1*$^{+/-}$ (**E''**) and *Arap1*$^{-/-}$ (**F''**). *Arrows* show filamentous Müller glial processes. *Arrowhead* shows Müller glial end feet surrounding retinal ganglion cell bodies in the inner retina. *Double arrowhead* shows staining in the OPL.
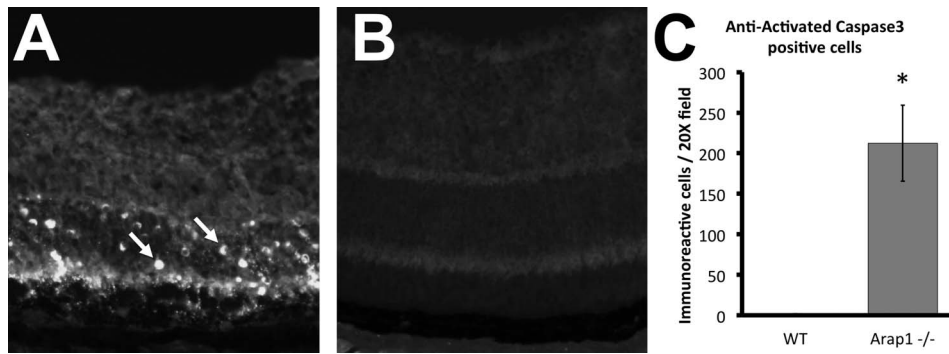
FIGURE 6. *Arap1^{−/−}* photoreceptors undergo programmed cell death. Immunohistochemistry using anti-activated Caspase-3 on adult (4 weeks) retinal sections of *Arap1^{−/−}* animals showed extensive staining in the ONL (**A**, *arrows*), indicative of widespread apoptosis in these photoreceptors. Control retinal sections from age-matched animals showed only the occasional apoptotic cell (**B**). Quantification of cell death at 4 weeks postnatal is shown in (**C**), with an average of 212.3 labeled cells per ×20 field in *Arap1^{−/−}* retina, and 1.7 labeled cells in wild-type retina. *Arap1^{−/−}* and wild-type retinal sections stained at 2 weeks and 8 weeks postnatal showed almost no apoptosis (data not shown) ($n = 3$ each group, *P < 0.05, *error bars* represent SE).

reasonable to posit that *Arap1* is required for photoreceptor survival by maintaining appropriate levels of EGFR signaling in the retina. Indeed, previous studies have shown that EGF and related ligands can stimulate proliferation of retinal progenitors in vitro.[9–13] However, careful analysis of EGFR-deficient mice showed that this receptor is required for only a modest degree of proliferation in late retinal progenitor cells, and no defect in rod photoreceptor development or survival was detected at any stage.[14] Given that rod cells develop and survive normally in EGFR^{−/−} mice, we reason that it is unlikely that the in vivo photoreceptor degeneration in *Arap1^{−/−}* animals is related to dysfunction in EGFR signaling.

We have not detected *Arap1* in photoreceptors, although we cannot exclude that it may be expressed at low levels. Although there is no known function of *Arap1* in photoreceptors, there is a known function for another Arf GAP of the AZAP family, *Asap1*, in rod photoreceptors.[15] *Asap1* acts on *Arf4* as its substrate to target rhodopsin to the rod outer segment. *Arf4* recognizes the VxPx outer segment localization sequence of rhodopsin, whereas *Asap1* binds rhodopsin's FR localization sequence. Many other small G-proteins (*Rab11, Rab8, Rab6*), GEFs (*Rabin 8, RPGR*), Arls, and Arl GAPs (*RP2*)

are present in the rod inner segment and participate in transport of rhodopsin to the outer segment through the connecting cilium (see Wang and Deretic[16] for review). *Asap1* functions as a scaffold for these soluble regulators of rhodopsin transport from the trans-Golgi network to the connecting cilium.[17] The presence of two GEFs, *Rabin 8* and *RPGR*, which both can act on *Rab8*, suggests the need for an exquisitely high level of regulation of rhodopsin trafficking to the outer segment. Therefore, it is plausible that *Arap1* represents another Arf GAP, in addition to *Asap1*, that serves to regulate *Arf4*. Based on the function of *Asap1* in rods, it is tempting to speculate that *Arap1* also regulates rhodopsin trafficking.

However, as there is no obvious expression in photoreceptors, this implies a cell nonautonomous mechanism for the requirement of *Arap1* for photoreceptor homeostasis. Most retinal degenerations are due to mutations in genes expressed in the dying photoreceptors. However, mutations in neighboring cells, such as RPE-specific genes, can be required for photoreceptor survival.[18–20] Although some expression by LacZ histochemistry is seen in the RPE, it is difficult to determine the degree of RPE expression in pigmented animals.
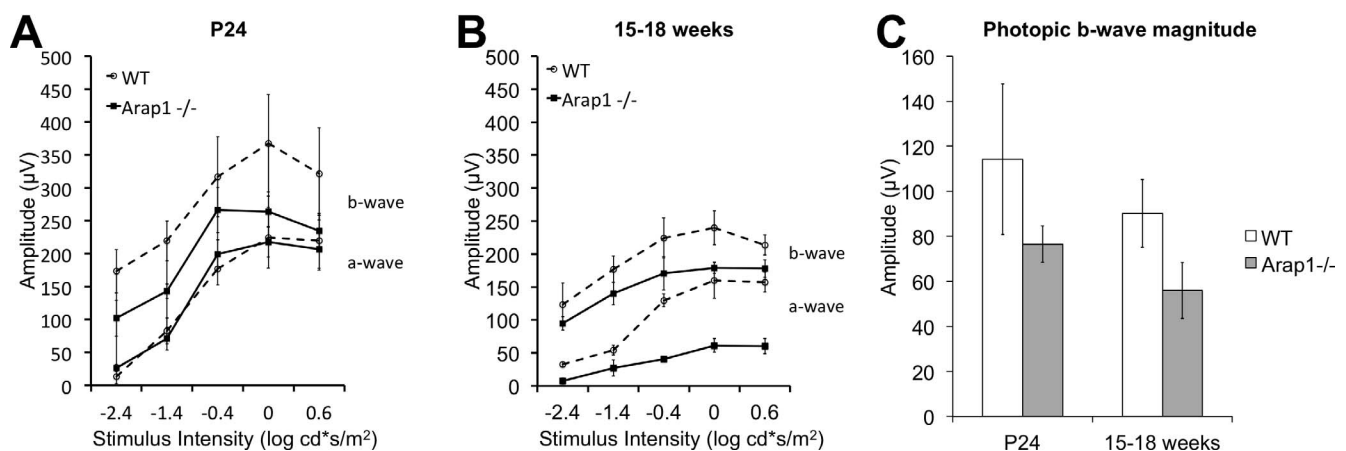

FIGURE 7. *Arap1^{−/−}* mice have reduced electrophysiologic function in rod and cone mediated pathways. Electroretinography (**A**) under dark-adapted conditions in *Arap1^{−/−}* animals at 24 days' postnatal age (*solid line*) show a normal a- and somewhat reduced b-wave in comparison with age-matched wild-type animals (*dashed line*). At later stages (15–18 weeks postnatal age), the scotopic a- and b-waves are significantly decreased (**B**) in *Arap1^{−/−}* animals compared with wild-type animals. The magnitude of the photopic b-wave (**C**) at the highest stimulus level (10 cd-s/m²) shows somewhat reduced, although not statistically significant, responses in *Arap1^{−/−}* animals at both 24 days' and 15 to 18 weeks postnatal age ($n = 3$ each group, *error bars* represent SE).

Investigative Ophthalmology & Visual Science

Arap1 is known to regulate the size of circular dorsal ruffles (CDR) in NIH 3T3 cells in vitro,[21] which are believed to facilitate bulk internalization of membranes or macropinocytosis.[22] *Arap1* was found to control CDR size via its Arf GAP function, binding to and activating the GTPase function of Arf1 and Arf5. ADP-ribosylation factor 1 is activated at the phagocytic cup[23] and is essential for phagocytosis.[24] It is possible that *Arap1* expressed in RPE cells regulates the physiologic diurnal phagocytosis of photoreceptor outer segments. Mutations altering the phagocytic function of the RPE resulting in photoreceptor degeneration have been described.[25] Further assays for the presence of ARAP1 protein and mRNA are necessary, likely on an albino background, to clarify its presence in the RPE.

We have detected β-galactosidase, a surrogate marker for *Arap1* expression, in Müller cells. Immunohistochemistry for β-galactosidase shows expression of protein in the same compartment as glutamine synthetase, within the cytoplasm of Müller glia. The LacZ histochemistry with X-gal reagent also shows a pattern consistent with Müller cell cytoplasmic compartments, which are largest at the end feet at the internal limiting membrane, in the inner retina, and at the external limiting membrane at the boundary between the outer nuclear layer and photoreceptor inner and outer segments. Single-cell transcriptome studies of Müller glia support the expression of *Arap1* (aka *Centd2*) in these cells.[26] Furthermore, next-generation sequencing analysis from mouse and human brain tissues suggest a predominantly glial expression profile of *Arap1* in the central nervous system.[27]

It is known that selective depletion of Müller glia leads to rod photoreceptor death,[28,29] but the mechanism of the dependence of photoreceptors on these cellular neighbors is unknown. Müller glia are involved in glucose metabolism and secrete ATP,[30] and photoreceptors are highly metabolic cells requiring constant supply of cellular energy.[31] Müller glia secrete numerous factors that may be required for photoreceptor neuroprotection, including CNTF, bFGF, PEDF, IGF-1, GDNF, VEGF, LIF, NGF, and BDNF.[32] The structural contribution of Müller glia to retinal architecture may be required for photoreceptor survival, as their processes form the external limiting membrane, a key boundary between photoreceptor nuclei and their inner and outer segments.[33,34] The ionic environment of the retina is regulated by Müller glia,[35] and they are implicated in vitamin A metabolism. Visual cycle genes are expressed in Müller glia, and it is known they participate in the visual cycle,[36] and perturbation of their role in regeneration of photopigment may lead to photoreceptor death. Further studies in Müller glia are necessary to determine the mechanisms by which they are required for photoreceptor survival.

The data presented here demonstrate that *Arap1*⁻/⁻ mice undergo photoreceptor degeneration strikingly similar to RP in humans; however, there is no recognized relationship between *Arap1* or related genes to humans with rod-cone dystrophies. Disruption of *Arap1,* and the pathways in which it is related to photoreceptors, is a novel and previously unknown cause of rod-cone dystrophy in mice. *ARAP1,* and/or its family members, may represent a new genetic locus responsible for a segment of human patients with RP. Although *ARAP1* mRNA is found in adult human retina at significant levels,[37] whole-genome sequencing in RP patients who do not have common disease-causing mutations is required to determine if *ARAP1* is clinically relevant in humans. We are not aware of any single gene mutation in Müller glia implicated in photoreceptor disease in humans or other vertebrates. Further studies are necessary to elucidate the role of *Arap1* in photoreceptor homeostasis and its clinical relevance to retinal disease.

References

1. Parmeggiani F. Clinics, epidemiology and genetics of retinitis pigmentosa. *Curr Genomics*. 2011;12:236–237.

2. Hamel C. Retinitis pigmentosa. *Orphanet J Rare Dis*. 2006;1: 40.

3. U.S. National Library of Medicine: Genetics Home Reference. Available at: https://ghr.nlm.nih.gov/condition/retinitis-pigmentosa#genes. Accessed June 1, 2016.

4. Saul SM, Brzezinski JA IV, Altschuler RA, et al. Math5 expression and function in the central auditory system. *Mol Cell Neurosci*. 2008;37:153–169.

5. Sun N, Shibata B, Hess JF, FitzGerald PG. An alternative means of retaining ocular structure and improving immunoreactivity for light microscopy studies. *Mol Vis*. 2015;21:428–442.

6. Miura K, Jacques KM, Stauffer S, et al. ARAP1: a point of convergence for Arf and Rho signaling. *Mol Cell*. 2002;9:109–119.

7. Campa F, Yoon HY, Ha VL, Szentpetery Z, Balla T, Randazzo PA. A PH domain in the Arf GTPase-activating protein (GAP) ARAP1 binds phosphatidylinositol 3,4,5-trisphosphate and regulates Arf GAP activity independently of recruitment to the plasma membranes. *J Biol Chem*. 2009;284:28069–28083.

8. Yoon HY, Lee JS, Randazzo PA. ARAP1 regulates endocytosis of EGFR. *Traffic*. 2008;9:2236–2252.

9. Anchan RM, Reh TA. Transforming growth factor-beta-3 is mitogenic for rat retinal progenitor cells in vitro. *J Neurobiol*. 1995;28:133–145.

10. Anchan RM, Reh TA, Angello J, Balliet A, Walker M. EGF and TGF-alpha stimulate retinal neuroepithelial cell proliferation in vitro. *Neuron*. 1991;6:923–936.

11. Lillien L. Changes in retinal cell fate induced by overexpression of EGF receptor. *Nature*. 1995;377:158–162.

12. Lillien L, Wancio D. Changes in epidermal growth factor receptor expression and competence to generate glia regulate timing and choice of differentiation in the retina. *Mol Cell Neurosci*. 1998;10:296–308.

13. Lillien L, Cepko C. Control of proliferation in the retina: temporal changes in responsiveness to FGF and TGF alpha. *Development*. 1992;115:253–266.

14. Close JL, Liu J, Gumuscu B, Reh TA. Epidermal growth factor receptor expression regulates proliferation in the postnatal rat retina. *Glia*. 2006;54:94–104.

15. Wang J, Morita Y, Mazelova J, Deretic D. The Arf GAP ASAP1 provides a platform to regulate Arf4- and Rab11-Rab8-mediated ciliary receptor targeting. *EMBO J*. 2012;31:4057–4071.

16. Wang J, Deretic D. Molecular complexes that direct rhodopsin transport to primary cilia. *Prog Retin Eye Res*. 2014;38:1–19.

17. Wang J, Morita Y, Mazelova J, Deretic D. The Arf GAP ASAP1 provides a platform to regulate Arf4- and Rab11-Rab8-mediated ciliary receptor targeting. *EMBO J*. 2012;31:4057–4071.

18. Ruiz A, Ghyselinck NB, Mata N, et al. Somatic ablation of the Lrat gene in the mouse retinal pigment epithelium drastically reduces its retinoid storage. *Invest Ophthalmol Vis Sci*. 2007;48:5377–5387.

19. Fan J, Rohrer B, Frederick JM, Baehr W, Crouch RK. Rpe65$^{-/-}$ and Lrat$^{-/-}$ mice: comparable models of leber congenital amaurosis. *Invest Ophthalmol Vis Sci*. 2008;49:2384–2389.

20. Duncan JL, LaVail MM, Yasumura D, et al. An RCS-like retinal dystrophy phenotype in mer knockout mice. *Invest Ophthalmol Vis Sci*. 2003;44:826–838.

21. Hasegawa J, Tsujita K, Takenawa T, Itoh T. ARAP1 regulates the ring size of circular dorsal ruffles through Arf1 and Arf5. *Mol Biol Cell*. 2012;23:2481–2489.

22. Buccione R, Orth JD, McNiven MA. Foot and mouth: podosomes, invadopodia and circular dorsal ruffles. *Nat Rev Mol Cell Biol*. 2004;5:647–657.

23. Beemiller P, Hoppe AD, Swanson JA. A phosphatidylinositol-3-kinase-dependent signal transition regulates ARF1 and ARF6 during Fcgamma receptor-mediated phagocytosis. *PLoS Biol*. 2006;4:e162.

24. Braun V, Deschamps C, Raposo G, et al. AP-1 and ARF1 control endosomal dynamics at sites of FcR mediated phagocytosis. *Mol Biol Cell*. 2007;18:4921–4931.

25. Mullen RJ, LaVail MM. Inherited retinal dystrophy: primary defect in pigment epithelium determined with experimental rat chimeras. *Science*. 1976;192:799–801.

26. Roesch K, Jadhav AP, Trimarchi JM, et al. The transcriptome of retinal Müller glial cells. *J Comp Neurol*. 2008;509:225–238.

27. Zhang Y, Sloan SA, Clarke LE, et al. Purification and characterization of progenitor and mature human astrocytes reveals transcriptional and functional differences with mouse. *Neuron*. 2016;89:37–53.

28. Byrne LC, Khalid F, Lee T, et al. AAV-mediated, optogenetic ablation of Müller Glia leads to structural and functional changes in the mouse retina. *PLoS One*. 2013;8:e76075.

29. Shen W, Fruttiger M, Zhu L, et al. Conditional Müller cell ablation causes independent neuronal and vascular pathologies in a novel transgenic model. *J Neurosci*. 2012;32:15715–15727.

30. Wang M, Wong WT. Microglia-Müller cell interactions in the retina. *Adv Exp Med Biol*. 2014;801:333–338.

31. Hurley JB, Chertov AO, Lindsay K, et al. Energy Metabolism in the Vertebrate Retina. In: Furukawa T, Hurley JB, Kawamura S, eds. *Vertebrate Photoreceptors: Functional Molecular Bases*. Springer Japan; 2014:91–137.

32. Vecino E, Rodriguez FD, Ruzafa N, Pereiro X, Sharma SC. Glia-neuron interactions in the mammalian retina. *Prog Retin Eye Res*. 2016;51:1–40.

33. Kohno T, Sorgente N, Ishibashi T, Goodnight R, Ryan SJ. Immunofluorescent studies of fibronectin and laminin in the human eye. *Invest Ophthalmol Vis Sci*. 1987;28:506–514.

34. Jerdan JA, Glaser BM. Retinal microvessel extracellular matrix: an immunofluorescent study. *Invest Ophthalmol Vis Sci*. 1986;27:194–203.

35. Uckermann O, Wolf A, Kutzera F, et al. Glutamate release by neurons evokes a purinergic inhibitory mechanism of osmotic glial cell swelling in the rat retina: activation by neuropeptide Y. *J Neurosci Res*. 2006;83:538–550.

36. Kaylor JJ, Yuan Q, Cook J, et al. Identification of DES1 as a vitamin A isomerase in Müller glial cells of the retina. *Nat Chem Biol*. 2013;9:30–36.

37. Pinelli M, Carissimo A, Cutillo L, et al. An atlas of gene expression and gene co-regulation in the human retina. *Nucleic Acids Res*. 2016;44:5773–5784.